Superconductivity in β-Phase Gallium

Hugo Parr and Jens Feder*
Fysisk Institutt, Universitetet i Oslo, Oslo, Norway
(Received 7 April 1972)

An experimental study of the superconducting properties of small single spheres of β-gallium has been made. Some spheres exhibited little superheating and went into the intermediate state so that $H_c(T)$ could be determined, giving $H_0 = 538 \pm 5$ Oe. The deviation of $H_c(T)$ from a parabolic temperature dependence is positive, indicative of strong-coupling superconductivity. T_c is 5.90 ± 0.03 K. For temperatures close to T_c, ideal superheating and supercooling is observed in the best spheres, allowing the determination of the Ginzburg–Landau parameter $\kappa = 0.141 \pm 0.002$. The variation with temperature of the signal difference between the superconductive and normal states determines the penetration depth of the magnetic field, giving $\delta_0 = 880 \pm 100$ Å. When the finite penetration depth is taken into account, agreement is obtained between the extrapolated values of $\kappa_{sc}(T)$ and $\kappa_{sh}(T)$ at T_c.

I. INTRODUCTION

In type-I superconductors, the phase transition between the normal and superconductive states is of the first order in the presence of a magnetic field. The phase diagram in the H-T plane for such a superconductor is illustrated in Fig. 1. At the thermodynamical critical field curve $H_c(T)$ the free energy of the normal and superconducting states are equal. However, under favorable conditions, one observes metastable states and a large hysteresis. Thus, in decreasing the magnetic field or the temperature from high values, the normal state transforms to the superconducting phase only when the supercooling field, i.e., the curve $H_{sc}(T)$, is reached. Similarly, the superconducting phase, although metastable outside the $H_c(T)$ curve, does not become intrinsically unstable until the superheating field $H_{sh}(T)$ is reached. In the metastable regions any kind of surface flaws will act as nucleation centers and tend to induce the thermodynamically stable phase. Thus "ideal" superheating and supercooling—i.e., the hysteresis characteristic of the material and not of the flaws—are rather difficult to achieve experimentally.

Faber[1] first studied systematically the supercooling field in various type-I materials. However, as he worked with bulk samples, he observed very little superheating. "Ideal" superheating was first seen in indium[2] by observing the transition in a powder sample containing many small spheres. A new phase cannot propagate in such a sample, a separate nucleation process being required in each sphere, and thus the limits of superheating and supercooling observed should represent the ideal case. This method has subsequently been used to investigate a number of materials.[2–13] The drawback of powder experiments is mainly that only relatively smeared-out transitions may be observed. This tends to make the interpretation of powder results difficult. Specifically, in the case of superheating, nonspherical particles with a demagnetization factor different from $\frac{1}{3}$ may dominate the tail end of the hysteresis loop and give a superheating field higher than it should be ideally for spherical particles. In the case of supercooling, the distortion of the static field by the particles which have already become superconducting may give erroneous results for the transitions of the remaining spheres. These problems are overcome by the study of superheating and supercooling in single spheres chosen under the microscope for their quality. This method has so far been used only for In,[14] Sn, and gold-plated In.[15] One advantage of this method is the fact that one can study the hysteresis as a function of field direction and thus obtain information as to the presence of invisible nucleation centers.[15] In the present paper we demonstrate that in single-sphere experiments

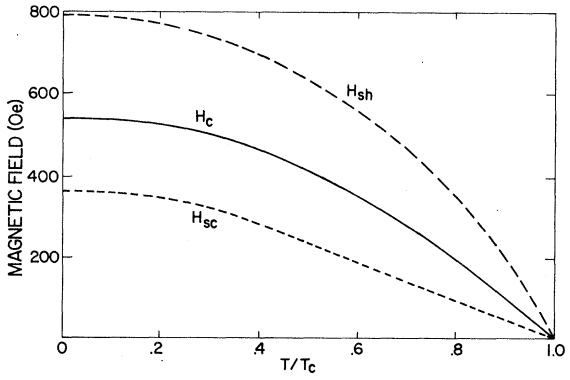

FIG. 1. Phase diagram of the superconducting-to-normal transition in β-Ga, based on observations made on single β-Ga spheres. H_c is the thermodynamic critical field. H_{sh} is the maximum superheating field for the superconducting state. H_{sc} is the minimum supercooling field for the normal state.

one can, in addition, measure the penetration depth of the magnetic field.

In our earlier experiments on gallium spheres[4] separated in frozen alcohol, we always found three different modifications present in the same sample: α, β, and γ, having transition temperatures of about $T_{c,\alpha} = 1.08$ K, $T_{c,\beta} = 6.2$ K, and $T_{c,\gamma} = 7.6$ K. Here we describe results obtained in single spheres of gallium not contained in any liquid. These were always found to solidify in the metallurgical β phase.

In Sec. II we summarize the theoretical background, and in Sec. III the experimental method is described. In Sec. IV we present the results for the reversible thermodynamic properties, the superheating and supercooling, and also for the size effects observed. In Sec. V we present a discussion of the results obtained.

II. THEORY

A. Signal

As described in Sec. III and seen in Fig. 2, we detect the superconducting-to-normal transition in the sphere by observing the signal induced in the pickup loop when a small alternating tickling field is applied to the primary. In the normal state the sphere is virtually transparent to the tickling field, whereas in the superconducting state the sphere can be considered to have an induced alternating dipole moment given by[16]

$$m = -\tfrac{1}{2}R^3\left[1 - 3\,\frac{\delta}{R}\left(\coth\frac{R}{\delta} - \frac{\delta}{R}\right)\right]h\,, \tag{1}$$

where h is the tickling field, R the radius of the sphere, and δ the penetration depth of the field into the superconductor. The change S in signal between the normal and superconducting states is thus proportional to m; the factor of proportionality depending upon the geometry of the pickup loop.

The penetration depth δ is temperature dependent, and it is customary to use the following form[17]:

$$\delta = \delta_0[1 - (T/T_c)^4]^{-1/2}\,, \tag{2}$$

which approximates very closely the Bardeen–Cooper–Schrieffer (BCS) temperature dependence except at very low temperatures. The zero-temperature penetration depth in the nonlocal regime $\lambda_L(0) \ll \xi_0$ is given by (Ref. 17, p. 174)

$$\delta_0 = \left(\frac{\sqrt{3}}{2}\,\frac{1}{\pi}\,\lambda_L(0)^2\xi_0\right)^{1/3}\,, \tag{3}$$

where the London penetration depth at zero temperature is

$$\lambda_L(0) = (mc^2/4\pi Ne^2)^{1/2}\,. \tag{4}$$

N is the number of electrons per unit volume. The zero-temperature coherence length is given by the BCS theory as

$$\xi_0 = 0.18\hbar v_F/kT_c\,, \tag{5}$$

where v_F is the Fermi velocity.

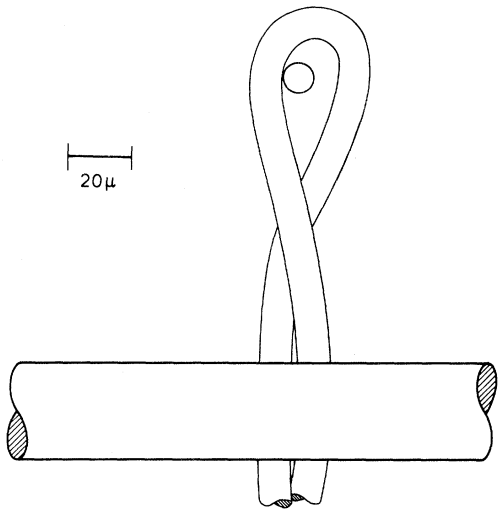

FIG. 2. Sample holder for the 11.5-μm β-Ga sphere described in the text, traced from a photograph. The proportions are not exact because only the sphere was in focus in the microscope. Secondary loop is made of 10-μm insulated Cu wire. Primary leads (only one is shown) are made of 30-μm insulated Cu wire. The substrate is copper. Sphere is lying freely in the loop.

We obtain the following result for the normalized signal change:

$$\frac{S(0) - S(T)}{S(0)} = \frac{(1 - \alpha + \tfrac{1}{3}\alpha^2) - (1 - \alpha y + \tfrac{1}{3}\alpha^2 y^2)}{1 - \alpha + \tfrac{1}{3}\alpha^2}\,, \tag{6}$$

where we have introduced

$$\alpha \equiv 3\delta_0/R \tag{7}$$

and

$$y \equiv [1 - (T/T_c)^4]^{-1/2}\,. \tag{8}$$

Equation (6) is appropriate in our case, when $\delta/R \ll 1$.

Thus, observing the change in signal in going from the superconducting to the normal state as a function of temperature, we may find δ_0, knowing R and fitting Eq. (6) to the results. This discussion is found in Sec. IV.

B. Supercooling

The superheating and supercooling are usually discussed in terms of Ginzburg–Landau (GL) theory.[18] Ginzburg[19] demonstrated that the bulk normal state is unstable with respect to the superconducting state whenever the field is less than

$$H_{c2} = \sqrt{2}\,\kappa H_c(T)\,, \tag{9}$$

where κ is the GL parameter. Gor'kov[20,21] has

shown that the GL parameter κ is given by

$$\kappa = 0.96\lambda_L(0)/\xi_0 \tag{10}$$

for a pure superconductor.

Saint-James and de Gennes[22] found that the instability of the normal state actually occurs at a higher field H_{c3} for the situation where the applied magnetic field is parallel to the surface of the superconductor. The supercooling field in this case is given by

$$H_{sc} = H_{c3} = 1.695\sqrt{2}\,\kappa H_c(T) . \tag{11}$$

For a sphere, one thus expects the normal state to become unstable at the equator where the applied field is parallel to the surface. The identification of H_{c3} with H_{sc} is valid only provided $\kappa < 0.409$, as pointed out by Feder.[23]

We shall, as usual, parametrize our observed supercooling fields by the parameter κ_{sc} defined by inverting Eq. (11), to give

$$\kappa_{sc} = 0.4172(H_{sc}/H_c) . \tag{12}$$

κ_{sc} is a purely experimental parameter which, however, is expected to approach the GL parameter κ as T_c is approached.

As discussed earlier,[15] close to T_c size effects set in which make κ_{sc} apparently diverge. One may estimate[19] that the size effect becomes important whenever

$$\xi_T = 0.74\xi_0(1 - T/T_c)^{-1/2} \geq 2R/7.5 . \tag{13}$$

C. Superheating

The superheating field H_{sh} may also be derived from the GL equations. However, the situation is more complicated since one must study the stability of a state with a finite order parameter, and thus the GL equations cannot be linearized. For $\kappa \ll 1$, the one-dimensional calculation gives[19,24]

$$H_{sh} = H_c/(\kappa\sqrt{2})^{1/2} , \quad \kappa \ll 1. \tag{14}$$

In the limit $\kappa \gg 1$, one finds $H_{sh} = H_c$ and numerical calculations have been performed for intermediate values of κ. The published numerical results[19,25] may be fitted rather accurately by

$$H_{sh} = [H_c/(\kappa\sqrt{2})^{1/2}](1 + 0.535\kappa) \tag{15}$$

for $\kappa < 0.8$.

Allowing fluctuations in the order parameter that may vary in more than one dimension, one will find lower instability fields. In particular one finds that $H_{sh} \to 0.75H_c$ instead of H_c as $\kappa \to \infty$.[26,27] We have also previously argued[15] that for $\kappa = 1/\sqrt{2}$, one should find $H_{sh} = H_c$, so that Eq. (14) should represent a good interpolation formula for the actual superheating field in the κ range of interest here.

The superheating field has unfortunately not been calculated for a spherical sample. It has been customary to simply use Eq. (14), multiplying the observed superheating field by $\frac{3}{2}$ to account for the demagnetizing field of the sphere. Thus, the experimental results are parametrized in terms of the superheating GL parameter κ_{sh} given by inverting Eq. (14) and including the factor $\frac{3}{2}$:

$$\kappa_{sh} = 0.3143(H_c/H_{sh})^2 . \tag{16}$$

We find, however, that a significant correction to Eq. (16) is obtained if one takes into account the finite penetration depth δ of the magnetic field into the sphere. The local equatorial field parallel to the surface of the sphere, H_0, is given by[16]

$$H_0 = \frac{3}{2}\left[1 - \frac{\delta}{R}\left(\coth\frac{R}{\delta} - \frac{\delta}{R}\right)\right]H , \tag{17}$$

where H is the applied field. In the limit $\delta/R \ll 1$, and with the notation of Sec. II A, we obtain

$$\kappa_{sh}^{(\delta)} = 0.3143(H_c/H_{sh})^2(1 - \tfrac{1}{3}\alpha y + \tfrac{1}{9}\alpha^2 y^2)^{-2} . \tag{18}$$

The importance of this correction is discussed in Secs. IV and V.

The GL theory is expected to hold only for $1 - T/T_c \ll \kappa^2$. For lower temperatures one should take into account the nonlocal electrodynamics of the superconductor. This has been attempted for the superheating field of a pure superconductor with the field parallel to the sample surface, with the result[8,12]

$$H_{sh} = 1.36H_c\kappa^{-1/3}(1 - t)^{-1/12} . \tag{19}$$

The evidence for such a nonlocal behavior is discussed in Sec. V.

III. EXPERIMENTAL

The spheres were produced by ultrasonic dispersion at 40 kHz of the molten metal. A cleaned glass tip was used on the ultrasonic drill to prevent contamination. Several liquids were tried as dispersants in order to obtain shiny, flawless surfaces. We obtained the best results by using a mixture of glycerol and alcohol in the proportions 2:1 by volume, to which was added 0.1% of KOH by weight. The exact proportions are not critical, but the presence of the base is important. After sonoration, the spheres were repeatedly rinsed in pure alcohol. The spheres thus produced ranged in size from 1 to 50 μm, with a distribution peak around 15 μm.

The metastable-phase β-Ga has a melting point of -16.3 °C,[28] and thus it is not possible to have solidified spheres at room temperatures. This creates considerable handling problems, as a liquid sphere very quickly develops flaws on contact with other spheres or with the supporting surfaces. Using a cold stage and a metallurgical microscope,

we could directly observe the solidification and remelting of droplets larger than 30 μm. The melting points and supercooled freezing temperatures that could be estimated agree with Bosio's values for the β and γ phases.

We could not distinguish the β and γ phases by microscope observation, but the superconducting transition temperature gives an unambiguous check, since Bosio *et al.*[29] were able to uniquely separate the superconductive properties of the β and γ phases by doing both superconductive and calorimetric measurements on the same powder samples. All of the 11 spheres we cooled down to liquid-helium temperatures turned out to be in the β phase.

The spheres were handled with a 30-μm-diam lacquer-insulated copper wire, attached to an x-y micrometer manipulator. They were selected under magnifications of 308 or 616, and transferred to the sample holder at a magnification of 110. All the spheres selected had shiny surfaces and no flaws on the visible part of the surface.

The diameter of the spheres was measured using a graduated eyepiece. This measurement could only be done to an accuracy of about $\frac{1}{2}$ μm, leaving considerable relative uncertainty in the size of the smaller spheres.

Our cryostat does not permit rapid insertion and cooldown of a sample, so that warmup to room temperature and remelting of the sphere were unavoidable. The spheres stayed at room temperature for a period of about 8 h before the final cooldown.

With small modifications, the detection system is the same as for the earlier single-sphere experiments,[14,15] and details have been published elsewhere.[30]

Figure 2 shows one of the best sample holders made. The pickup loop was connected to the primary of a toroidal transformer with a stepup ratio of 1000. The secondary was connected to the input of a PAR H-8 lock-in amplifier, acting as a resonant circuit with a frequency of 76 kHz and a Q factor of 4 at liquid-He temperatures. The output of the lock-in was fed to an x-y recorder.

The signal-to-noise ratio obtained in this system depends rather critically on loop size and the position of the sphere in the loop. It is roughly proportional to $(1/D_1)(1/D_2)$, where D_1 is the mean loop diameter and D_2 is the distance from the sphere center to the closest part of the loop. It is therefore advantageous to place the sphere close to the loop perimeter and not in the middle. We have made a rough estimate of the pickup loop signal induced as a result of the normal-to-superconducting transition of the 11.5-μm sphere in Fig. 2, for a tickling field of frequency 75 kHz and peak-to-peak amplitude 0.3 Oe at the sphere. We find

$$V \cong 3\times 10^{-10}\ V\ .$$

To arrive at this figure, the pickup loop has been approximated by a circular loop of diameter 35 μm concentric with the sphere. This figure must be considered an upper limit to the real signal. Figure 3 shows an actual recorder trace for the transition of this sphere. At temperatures so close to T_c that the tickling field was not negligible compared to H_{sc} and H_{sh}, measurements were routinely carried out for two different tickling fields, and the result extrapolated to zero tickling field, giving the correct values for H_{sc} and H_{sh}.

The cryostat used had separate inner and outer baths of liquid He^4. All electrical leads were thermally anchored in both baths. The copper sample holder was placed inside a vacuum jacket and connected to the inner bath by a thermal resistance of about 0.0005 W/K.

A germanium thermometer (Honeywell) was placed in a hole in the copper sampleholder. Thermal contact was provided by Apiezon N grease and Ge-7031 varnish.

The thermometer was calibrated in the range

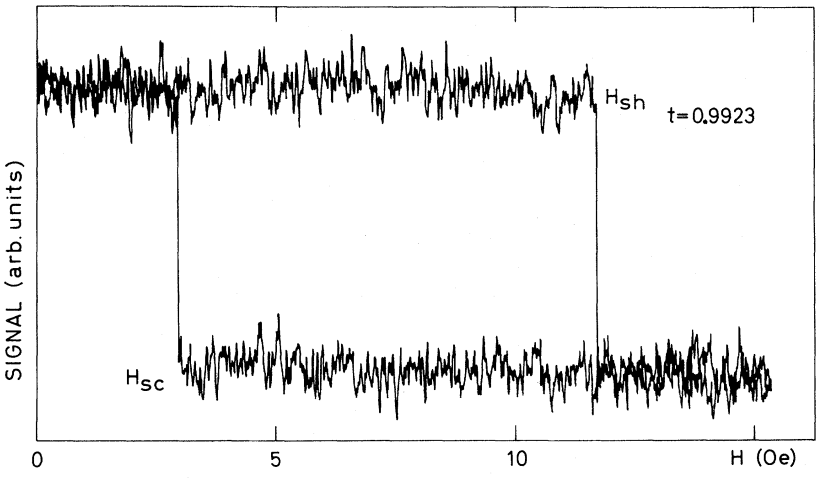

FIG. 3. Recorder trace of superconductive superheating and supercooling in β-Ga sphere of diameter 11.5 μm. Time constant of the lock-in amplifier is 300 msec. Noise amplitude corresponds to 20 nV at amplifier input.

0.5–1.4 K against He^3 vapor pressure, in the range 1.4–4.2 K against He^4 vapor pressure, and in the range 4.2–10 K against a factory calibrated germanium resistance thermometer (Cryocal). We believe the absolute error in our temperature readings to be less than 8 mK in the range 1.0–4.2 K, and less than 30 mK in the range 4.2–10 K. Relative temperatures for a single run are known everywhere to an accuracy better than 2 mK, except for the region of overlap at 4.2 K where the error may be slightly larger.

A sphere's response to temperature changes as seen from the superheating and supercooling fields came within a fraction of a second, indicating a good thermal contact to the sample holder.

The main static magnetic field was generated by a small fixed copper solenoid. The earth's magnetic field was shielded by a long cylinder of μ-metal placed around the cryostat. This reduced the axial component of the earth's field to about 0.07 G at the sample. The transverse component was only a fraction of this.

After a number of field sweeps, an axial remanent field of about 0.2 G always developed, presumably owing to superconductive flux trapping in various parts of the cryostat. To correct for this remanent field, field sweeps were carried out in two opposite directions of the static field and the results averaged.

The circular sample holder could be rotated around an axis perpendicular to the static field by means of a tight 0.13-mm stainless-steel wire running twice around the sample holder and fastened at both ends to a brass wheel at room temperature.

IV. RESULTS

We have investigated 11 single spheres of β-Ga, with diameters ranging from 7 to 26 μm. We only present the results for the best and/or the most illustrative samples.

A. Transition Temperature T_c

For each sphere, the transition temperature was determined in three different ways: (a) by sweeping the temperature with the sphere in zero external field, determining the point where the superconductive signal disappears; (b) by extrapolating the observed superheating and supercooling fields to zero; (c) by picking T_c so the $\kappa_{sh}(T/T_c)$ and $\kappa_{sc}(T/T_c)$ both show a size effect starting at the same value of T/T_c. Method (c) was the method used in the previous single-sphere experiments on indium and tin.[14,15] It is a very sensitive method, determining T_c to about 1 mK.

For any particular sphere investigated, these three methods gave results agreeing within 5 mK. Methods (b) and (c) consistently gave transition temperatures 2–4 mK higher than the direct method (a), which, however, had an uncertainty of this order of magnitude owing to the difficulty of observing high-temperature tails indicative of the rapidly waning superconductive state.

The T_c thus measured varied from one sphere to the next, presumably because of irreproducibility of the thermometer and its thermal anchoring. Our weighed result is

$$T_c = 5.90 \pm 0.03 \text{ K} .$$

Earlier determinations include that of Bosio *et al.*[28] who determined T_c from powder experiments extrapolating $H_c(T^2)$ from 4.2 K. Their result, 6.0 ± 0.1 K, is in fair agreement with the present more accurate value. Feder *et al.*,[4] also studying powders, found 6.2 ± 0.1 K. The cryostat used was, however, rather unsuited for measurements above 4.2 K, and the error may have been larger than indicated.

In these powder experiments, the particles were frozen in a solution of sodium oleate in ethyl alcohol, which solidifies around $-70\,^{\circ}$C. Thus the liquid solidifies before most of the particles. Upon solidifying in this solid matrix, the particles may well be severely strained, and this may explain the different T_c's reported.

B. Thermodynamic Critical Field $H_c(T)$

Some of the single spheres investigated exhibited poor supercooling and superheating because of defects. We also found that spheres remelted and kept at room temperatures for a period of several days always showed less hysteresis upon reinvestigation. In this way, even though superheating was always present, the superheating field H_{sh} would sometimes be less than H_c so that the sphere would go into the intermediate state when the field was increased above H_{sh}. For the largest sphere, of diameter 26 μm, the intermediate state could be observed at all temperatures below $T/T_c = 0.926$. A recorder trace of a field sweep for this sphere is shown in Fig. 4. If the field sweep is stopped after the superheating transition has occurred, the sphere is in the intermediate state and further increase or decrease of the field will trace out a reversible curve joining the Meissner state to the normal state. If, however, the field increases above H_c, supercooling will occur upon decreasing the field. Thus H_c can be accurately measured. If the system is in the intermediate state and the field is lowered below the demagnetizing field $H_D = (1 - D)H_c$ where D is the demagnetization factor, it will superheat when the field is increased again. Thus, in one sample one can observe superheating, supercooling, and reversible behavior. The intermediate-state curve is reproducible and the irregular structure corresponds to flux movements. This sample has a ratio of major-to-minor axis

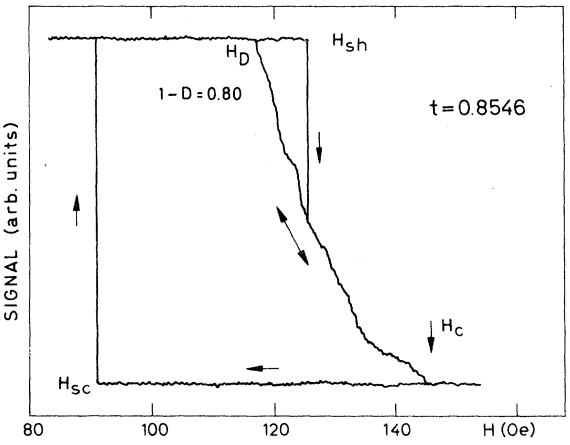

FIG. 4. Recorder trace for 26-μm β-Ga sphere showing both irreversible and reversible superconductive transitions in the region far from T_c. H_{sh} and H_{sc} are the superheating and supercooling fields. H_D is the demagnetizing field defined by $H_D=(1-D)H_c$, where D is the demagnetizing coefficient. From such data, $H_c(T)$ was determined as explained in Sec. IV B.

close to 1.5, and a demagnetization factor $D=0.2$, as observed in Fig. 4, is to be expected.

These measurements of $H_c(T)$ are precise enough to see a definite deviation from a parabolic temperature dependence. In Fig. 5 we have plotted the results for $H_c(T)$ as a normalized deviation from a T^2 dependence. All these measurements were performed on the 26-μm sphere, and T_c for this sphere was determined by a temperature sweep in zero field. The few measurements of H_c done on smaller spheres at low temperatures are consistent with the results on the large sphere. The uncertainty in the determination of T_c has been converted into a corresponding uncertainty in H_c, indicated in the figure as the error bar at the open circle at $t=1$. The open triangles in Fig. 5 are measurements of H_c in the size-effect region, and will be discussed later. We conclude from these measurements that

$$H_0 = 538 \pm 5 \text{ Oe}$$

and that the deviation $D(t) = (H_c/H_0) - (1 - t^2)$ is *positive* with a maximum value $D(t)_{max} = +0.008 \pm 0.003$.

We note that $D(t)$ changes sign at high temperatures. This may be a real effect or a consequence of the limited accuracy of the factory-calibrated thermometer used as a secondary standard in the region of T_c.

In Fig. 6, the present results for $D(t)$ on β-Ga are shown, together with results published by other authors on Hg[31] and α-Ga.[32,33] The weak-coupling BCS theoretical curve[34] is also drawn for comparison. There is a striking difference between α-Ga and β-Ga, the curve for β-Ga being more similar to the Hg curve than to any weak-coupling superconductor.

Bosio *et al.*[29] have previously determined H_0 in their powder experiments. They found 560 ± 5 Oe, which is 4% above our present value. Here again, one should keep in mind that the powder experiments were performed on particles embedded in ethyl alcohol. The ensuing pressure and strain effects may explain the higher values of $H_c(T)$ and T_c obtained from powder experiments.

C. "Mixed State" near T_c

Close to T_c the 26-μm sphere deviated from bulk behavior. For this sphere, one could distinguish three temperature regions:

$t < 0.926$. In this domain, $H_{sh} < H_c$, permitting observation of H_c and H_D as described in Sec. IV B. H_D/H_c is about constant for all temperatures, equaling 0.80.

$0.926 < t < 0.988$. In this region, $H_{sh} > H_c$, and only clean, square hysteresis loops could be observed.

$t > 0.988$. In this region, the superheating was again reduced and reversible behavior indicative of size effects could be observed, as explained in the following.

Figure 7 shows a recorder trace for the 26-μm sphere in the region close to T_c. Two distinct hysteresis loops are apparent, as well as a reversible curve. The change with temperature of the fields

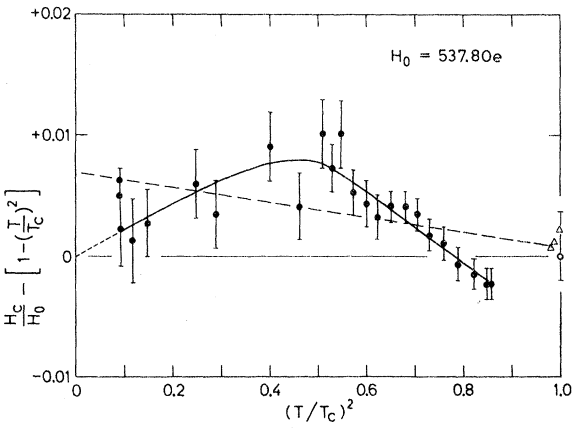

FIG. 5. Experimental results for $H_c(T)$ for the 26-μm sphere of β-Ga, obtained in three different cooldowns. Results are presented as a deviation from a parabolic temperature dependence. Solid dots are measurements of $H_c(T)$ from recorder traces of the type shown in Fig. 4. Open circle represents the experimental transition temperature T_c (see text). Open triangles represent measurements of $H_c'(T)$ in the size-effect region, obtained from recorder traces of the type shown in Fig. 7. Dotted line is the parabolic least-squares fit used in the computation of $\kappa_{sc}(t)$ and $\kappa_{sh}(t)$. Solid curve gives our proposed temperature dependence of $D(t) = H_c(t)/H_0 - (1-t^2)$.

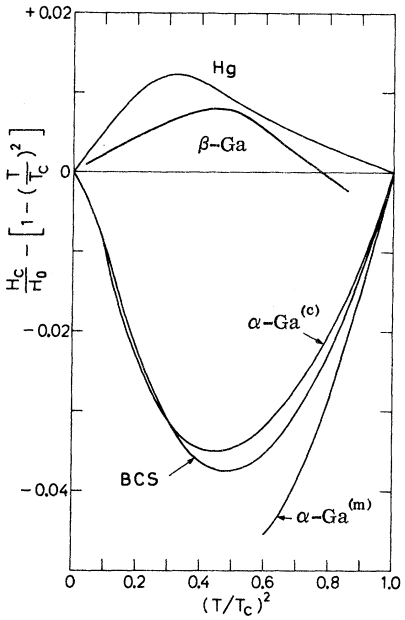

FIG. 6. Experimental results for $H_c(T)$ for β-Ga are compared to earlier results on α-Ga, Hg, and theoretical BCS weak-coupling prediction. Superscripts refer to calorimetric measurements (c), and magnetic measurements (m). Data on Hg are from Mapother (Ref. 31), on α-Ga$^{(c)}$ from Phillips (Ref. 32), on α-Ga$^{(m)}$ from Gregory *et al.* (Ref. 33), and on BCS from Swihart (Ref. 34).

labeled H_{sh} and H_{sc} shows that they develop smoothly from the bulk superheating and supercooling at lower temperatures. The field H_c' must be interpreted as the thermodynamic critical field for the sphere at this temperature. Our data indicate that it may be slightly larger than the bulk H_c. The resulting dH_c'/dT^2 is 7% lower than dH_c/dT^2. In all probability, H_c' arises from a size effect in the critical field.

The most interesting feature of the curve in Fig. 7 is the appearance of a new field H_1. Experimentally, we were never able to prevent the sphere from going completely into the Meissner state once the field was decreased below H_1. The ratio H_1/H_c' varied from 0.53 to 0.07 as the temperature increased from $t=0.986$ to $t=0.999$. H_1, therefore, clearly has no connection to the demagnetizing field H_D seen at low temperatures, since the observed H_D/H_c is expected to increase as T_c is approached because of the increasing penetration depth. It is tempting to identify the transition at H_1 as similar to that occurring at H_{c1} for type-II superconductors. Between H_1 and H_c', the sphere might then be in a state analogous to the mixed state for type-II superconductors. Other authors[35] have shown that thin films of type-I material can exhibit a vortex state if $D<\xi(T)$.

D. Superheating and Supercooling

The main purpose of this work was to investigate the superheating and supercooling properties of β-Ga, since the earlier experiments performed on powders in frozen ethyl alcohol[4] gave results indicating a large difference between κ_{sc} and κ_{sh}.

As discussed in Sec. II, we choose to present our experimental results parametrized in the usual way, in terms of κ_{sc} [see Eq. (12)], κ_{sh} [see Eq. (16)], and κ_R:

$$\kappa_R = 0.3780(H_{sc}/H_{sh})^{2/3}. \tag{20}$$

Here, κ_R is obtained by eliminating H_c from the equations for κ_{sc} and κ_{sh}. The spherical demagnetizing coefficient has been included in κ_{sh}. Of the three parameters, κ_R is the easiest to determine accurately from experiment, since it depends only on H_{sh} and H_{sc}. Computation of the other parameters requires knowledge of H_c, which cannot be experimentally determined for the best spheres. One finds that κ_{sh} and κ_{sc} near T_c, are strongly influenced by the precise choice of T_c, whereas κ_R is not.

For $H_c(T)$, we use our own measured values, presented in Sec. IV B. However, we do not find it necessary to take account of the correction $D(t)$ to a parabolic temperature dependence, since this correction is so small. Instead, we use the computer least-squares parabola fit to our data for $H_c(T)$, indicated by a broken line on Fig. 5. The error in making this approximation is nowhere larger than 0.8%. The equation for the straight line used is

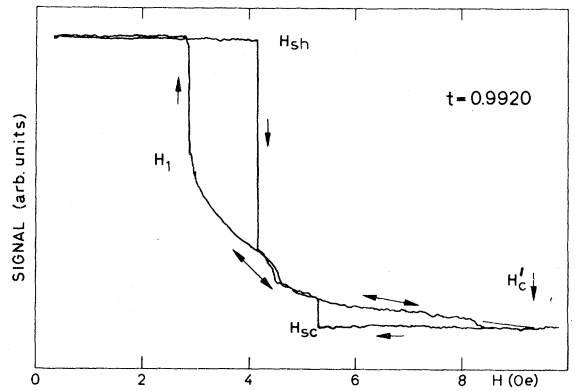

FIG. 7. Recorder trace of reversible and irreversible superconductive transitions for a 26-μm β-Ga sphere in the region very close to T_c. In addition to the superheating and supercooling fields also shown in Fig. 4, a new field H_1 is observed, giving rise to a double hysteresis loop. Extrapolation to H_c' is justified by doing this sweep for several different tickling fields.

$$\tilde{H}_c(T) = \tilde{H}_0[1 - (T/T_c)^2] , \quad (21)$$

where $\tilde{H}_0 = 541.6$ Oe and T_c is determined separately for each sphere.

Of the three possible methods outlined in Sec. IV A to determine T_c for a given sphere, we have adopted method (c) for the presentation of the supercooling and superheating results. Figure 8 shows $\kappa_{sh}(t)$ and $\kappa_{sc}(t)$ for the 11.5-μm sphere with T_c picked so that both curves have similar minima at $t \simeq 0.99$. It must be stressed that if we had used T_c of method (a) instead of T_c of method (c), neither this sphere nor the other good spheres would show any size effect at all in κ_{sh}.

Figure 9 shows $\kappa_R(t)$ for the three best spheres of β-Ga. The 13-μm sphere is clearly not as good as the other ones, but if we extrapolate $\kappa_R(t)$ to $t = 1$, neglecting the size effects, the values for all three spheres are comparable. Note the shift in the minimum with decreasing sphere size. The minima occur approximately at $t = 0.9950$, 0.9895, and 0.9860 for the 13-, 11.5-, and 7-μm spheres, respectively. In contrast to the curves for κ_{sh} and κ_{sc}, these curves are completely insensitive to the exact value of T_c.

Returning to Fig. 8, showing $\kappa_{sc}(t)$ and $\kappa_{sh}(t)$ for the 11.5-μm sphere, we notice that the curves cross at about $t = 0.96$. For $t > 0.96$, κ_{sh} is less than κ_{sc}. The extrapolated values to $t = 1$ are quite different for the two curves if we base the extrapolation on the region $0.95 < t < 0.99$. This feature is present for *all* of the best spheres investigated. $\kappa_{sc}(t)$ and $\kappa_{sh}(t)$ for the two best spheres are shown in Figs. 10 and 11, respectively.

In light of the good agreement obtained between the extrapolated values of $\kappa_{sc}(t)$ and $\kappa_{sh}(t)$ for other metals,[2-15] it seemed strange that a clear discrepancy should occur for β-Ga. This led us to consider the effect of a non-negligible penetration depth $\delta(T)$ of the magnetic field into the sphere, as explained in Sec. IIC. Our results for the penetration depth of β-Ga are presented in Sec. IV E. We shall see that when the ensuing corrections are taken into account, the obtained values of κ_{sh} have to be increased significantly.

In view of these doubts raised about the interpretation of the superheating data, we choose to determine the GL parameter κ by extrapolation of the supercooling results. We should first, however, satisfy ourselves that we have observed ideal metastable states. Evidence for this can be found in the rotational diagrams for the two best spheres, Figs. 12 and 13. For the 7-μm sphere, there is considerable structure in κ_{sc} at $t = 0.760$, indicating that defects prevent observation of the ideal limit of metastability. But for all temperatures above $t = 0.90$, this structure has essentially faded away, indicating that we are close to ideal conditions, the coherence length having become large enough to prevent these defects from acting as nucleation centers. The corresponding curves for κ_{sh} show considerably more structure, even at the highest temperatures. The angular dependence of κ_{sc} for 11.5-μm sphere shows a somewhat larger variation with angle than for the 7-μm sphere. At $t = 0.392$, the effect of the defects is clearly seen. The corresponding structure is fading out at $t = 0.951$. Above this temperature, only a small residual variation is left. Most of the variation in κ_{sc} above $t = 0.95$ may be considered to be "noise" owing to the experimental uncertainty in κ_{sc} which grows rapidly as one get close to T_c. The main series

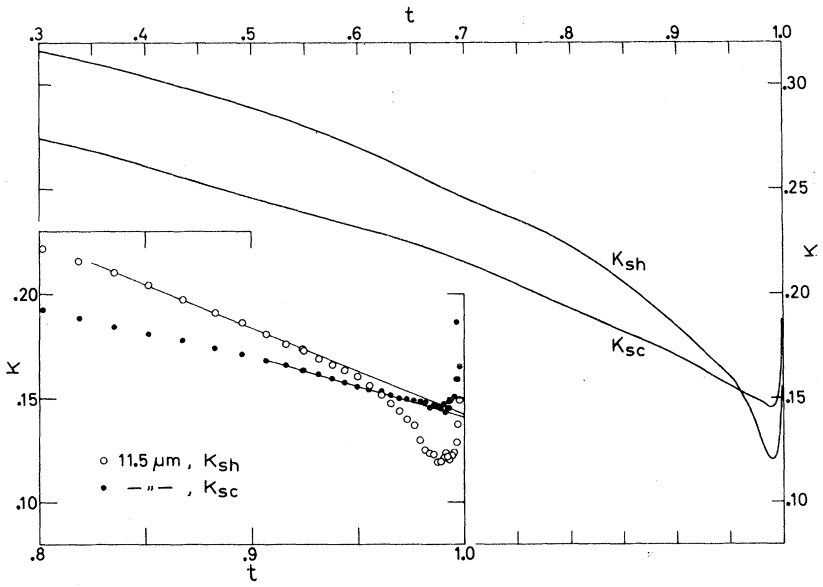

FIG. 8. Experimental results for $\kappa_{sh}(t)$ and $\kappa_{sc}(t)$ for the best β-Ga sphere investigated, of diameter 11.5 μm. Insert is a blowup of the region close to T_c, showing the actual experimental points. The GL parameter $\kappa(t = 1)$ is determined from an extrapolation of $\kappa_{sc}(t)$ to $t = 1$, neglecting the size-effect increase close to T_c, as explained in the text.

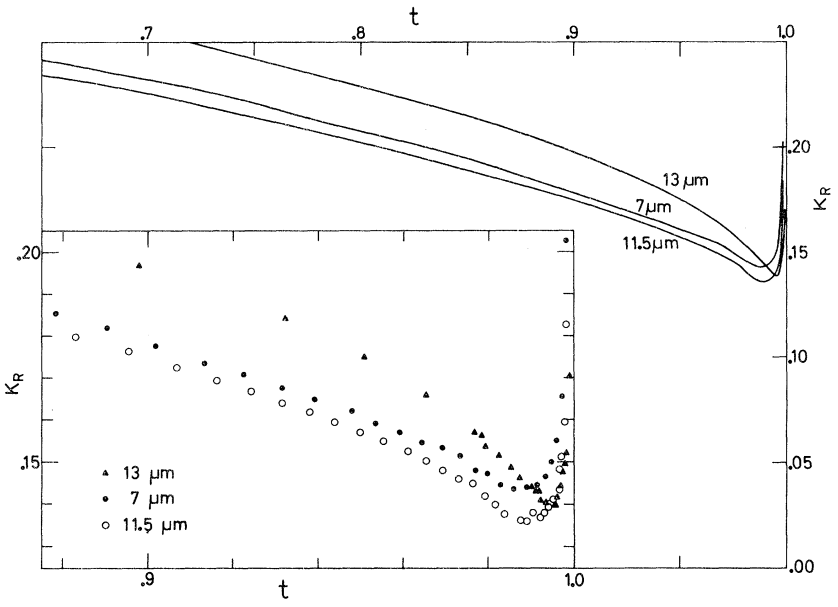

FIG. 9. $\kappa_R(t)$ for the three best β-Ga spheres investigated. Insert is a blowup of the region close to T_c. Notice how the minimum in the curve goes farther away from T_c with decreasing sphere diameter. The 13-μm sphere is clearly of poorer quality than the two others.

of measurements for the 11.5-μm sphere (see Figs. 8–11) has been carried out in the field direction of maximum supercooling, indicated by an arrow in Fig. 13. We are confident that this series gives ideal supercooling in the region approximately above $t = 0.90$.

In conclusion, we will determine the GL parameter κ for β-Ga by extrapolating the curves for $\kappa_{sc}(t)$ to $t = 1$. Figure 10 shows $\kappa_{sc}(t)$ for the two best spheres investigated. The extrapolated value of $\kappa_{sc}(t)$ does not depend very strongly on the exact choice of T_c, since only points in the region $t < 0.975$ are used. From the extrapolation of $\kappa_{sc}(t)$ for the 11.5-μm sphere, we obtain a GL parameter

$$\kappa_{sc}(t=1) = \kappa(t=1) = 0.141 \pm 0.002 \ .$$

In the previous powder experiment, Feder *et al.*[4] found $\kappa_{sc}(1) = 0.13$ and $\kappa_{sh}(1) = 0.18$. No error is quoted. In that experiment large errors were induced by the fact that temperatures could not be stabilized. Moreover, $H_c(T)$ was not accurately known.

The slope of $\kappa_{sc}(T)$ at T_c is of some theoretical interest, and we find

$$\frac{1}{\kappa}\left(\frac{\partial \kappa}{\partial t}\right)_{t=1} \cong -1.9 \pm 0.1 \ ,$$

whereas the theoretical estimate[36] gives the value

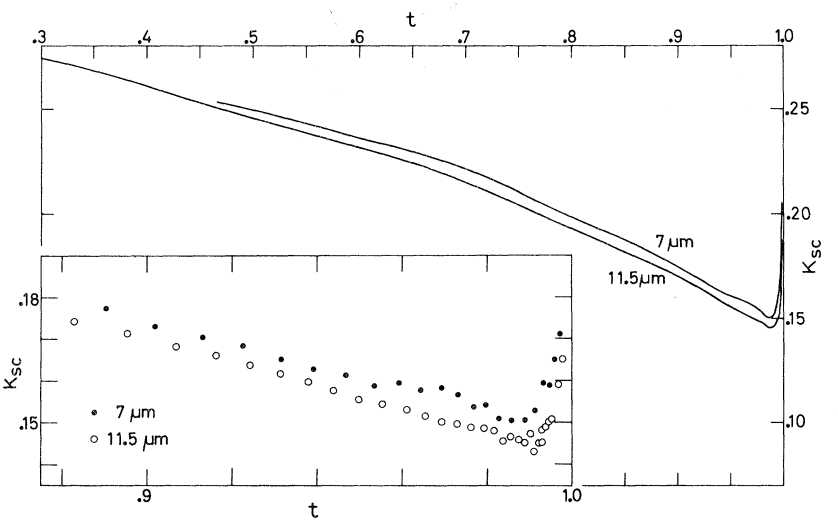

FIG. 10. $\kappa_{sc}(t)$ for the two best β-Ga spheres investigated. Insert is a blowup of the region close to T_c.

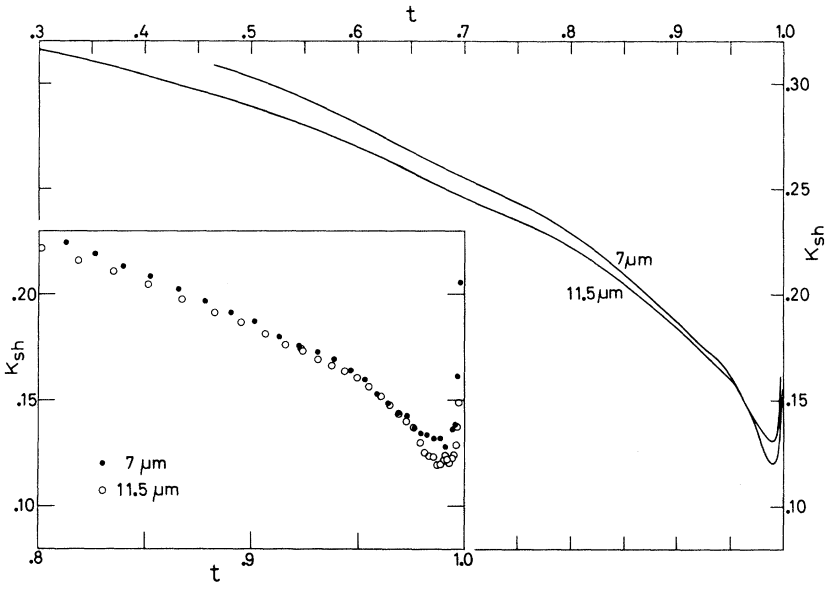

FIG. 11. $\kappa_{sh}(t)$ for the two best β-Ga spheres investigated. No corrections for penetration depth have been made. Notice the apparent "knee" in the curves at about $t = 0.945$. When the correction for the penetration depth is applied, this knee is seen to be somewhat smoothed out (see Fig. 15).

-1.0. The experimental value is certainly only an upper limit, as flaws will always tend to increase this slope. For spheres of lesser quality, the above quantity was often found to be two or three times as large.

In the earlier single-sphere experiments,[14,15] a symmetry was observed in the rotational diagrams of tin spheres, indicating an anisotropy in κ_{sh} and κ_{sc}. No such symmetry is seen in β-Ga, as evidenced by Figs. 12 and 13.

E. Size Effects

As discussed in Sec. IIA, the change in signal between the normal and superconducting states may be used to obtain a quantitative measure of the penetration depth δ.

In Fig. 14 the observed temperature dependence of the normalized signal depression is plotted versus $y = (1 - t^4)^{-1/2}$ for the 7- and the 11.5-μm spheres. The solid curves were obtained by a least-squares fit to the theoretical expression [Eq. (6)] of the data for the 11.5-μm sphere. Only the data for which $y < 8.5$ were used, the position of the remaining points being strongly dependent upon the precise value of T_c chosen. The least-squares fit gave

$$\alpha = 3\delta_0/R = 0.046$$

and a magnetic field penetration depth at zero temperature,

$$\delta_0 = 880 \pm 100 \text{ Å}.$$

Using this value of δ_0, the theoretical curve for the 7-μm sphere was calculated and, as seen in Fig. 14, the fit to the experimental data is rather good.

Theory predicts that the penetration depth should also be field dependent. As the order parameter at the surface is reduced by the increasing field, one would expect to measure a zero-temperature penetration depth[12,24]

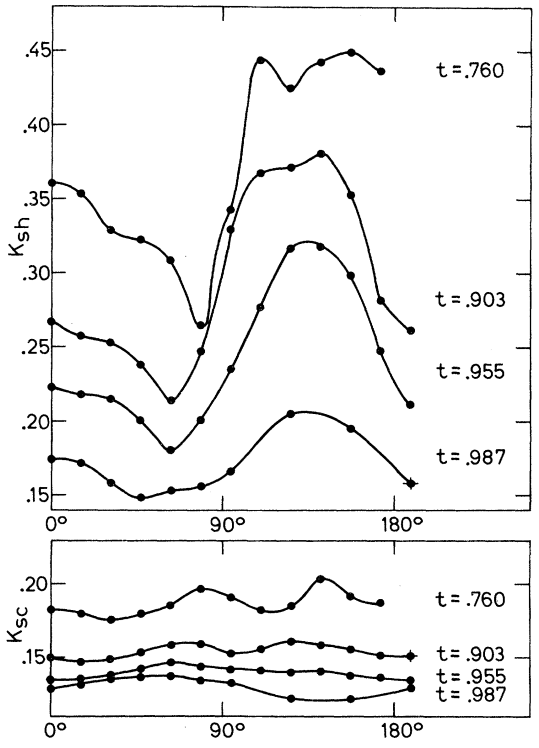

FIG. 12. $\kappa_{sh}(t)$ and $\kappa_{sc}(t)$ as a function of field orientation for the 7-μm sphere of β-Ga, for four different temperatures.

$$\delta_s = \delta_0(\psi_s/\psi_0)^{-2/3} , \tag{22}$$

if the tickling field is parallel to the static field. At the superheating field, theory predicts that

$$\psi_s/\psi_0 = 1/\sqrt{2} \quad (H = H_{sh}) . \tag{23}$$

The tickling field was not parallel to the static field in our experiment. We found no magnetic field dependence of δ to within 2%; i.e., the changes in signal for the superheating and the supercooling transitions were equal within experimental error.

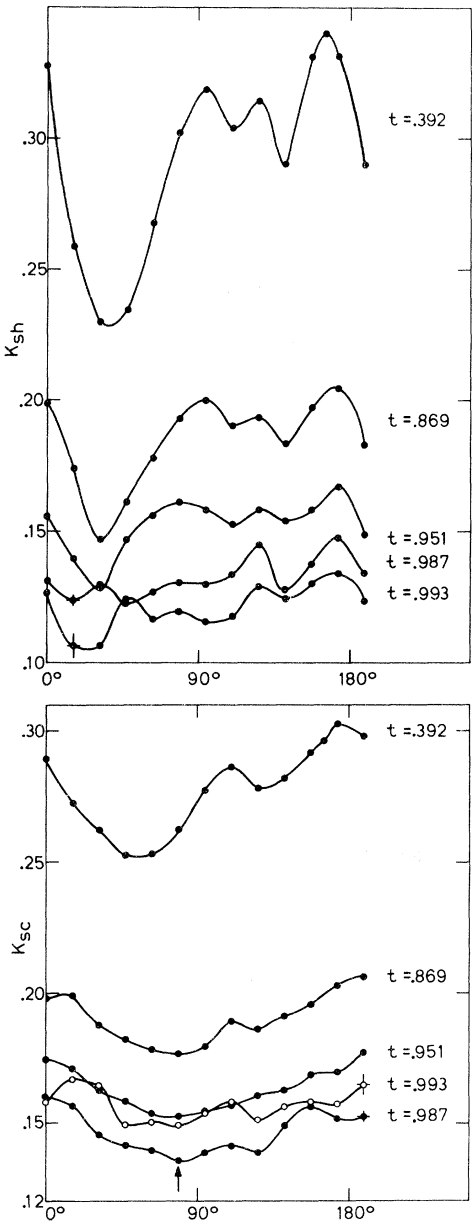

FIG. 13. $\kappa_{sh}(t)$ and $\kappa_{sc}(t)$ as a function of field direction for the 11.5-μm sphere of β-Ga, performed for five different temperatures. Error bars are given for temperatures close to T_c. At lower temperatures the error is less than the extension of the dot.

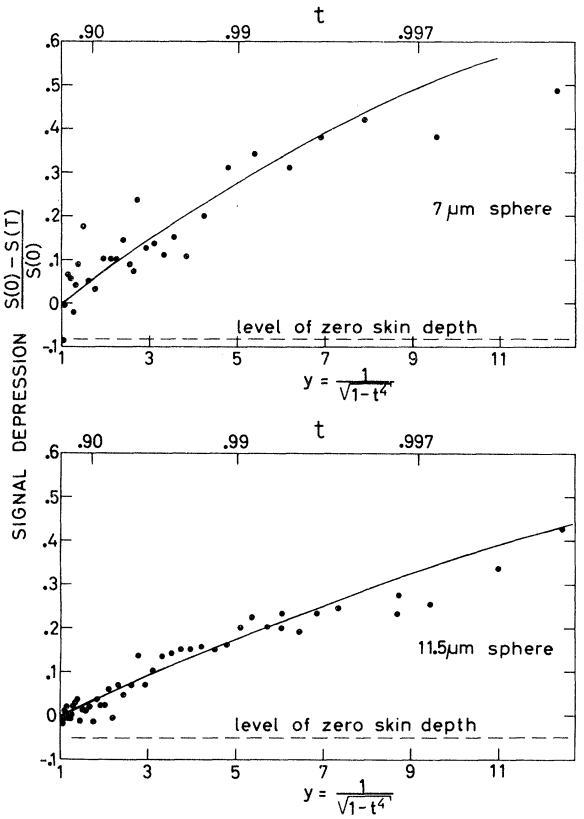

FIG. 14. Normalized signal depression $[S(0)-S(T)/S(0)]$ for the 11.5- and 7-μm spheres of β-Ga plotted vs $y = (1-t^4)^{-1/2}$. The solid curve for the 11.5-μm sphere is a least-mean-squares fit to Eq. (6), giving $\delta_0 = 880$ Å. The solid curve for the 7-μm sphere is obtained with the same δ_0, by scaling the radii. Dotted horizontal line indicates the signal amplitude for the hypothetical case of zero penetration depth.

We are now in a position to calculate the corrected κ_{sh}, taking into account the finite penetration depth, by using Eq. (18) with $\alpha = 0.046 \times 2^{1/3} = 0.058$. The factor $2^{1/3}$ comes from the depression of the surface order parameter, Eqs. (22) and (23). The resulting κ_{sh} values for the 11.5-μm sphere are presented in Fig. 15. The correction due to the finite penetration depth is seen to be quite large. In fact, the discrepancy between κ_{sh} and κ_{sc} in the region close to T_c has been removed, the remaining difference being within experimental error.

Having measured κ and δ_0, we can make use of Eqs. (3) and (10) to obtain $\lambda_L(0)$ and ξ_0. It should be remembered that Eq. (3) is derived assuming a plane boundary, and one may expect δ_0 for a sphere to be larger. However, as the equations for the spherical geometry have not been solved,

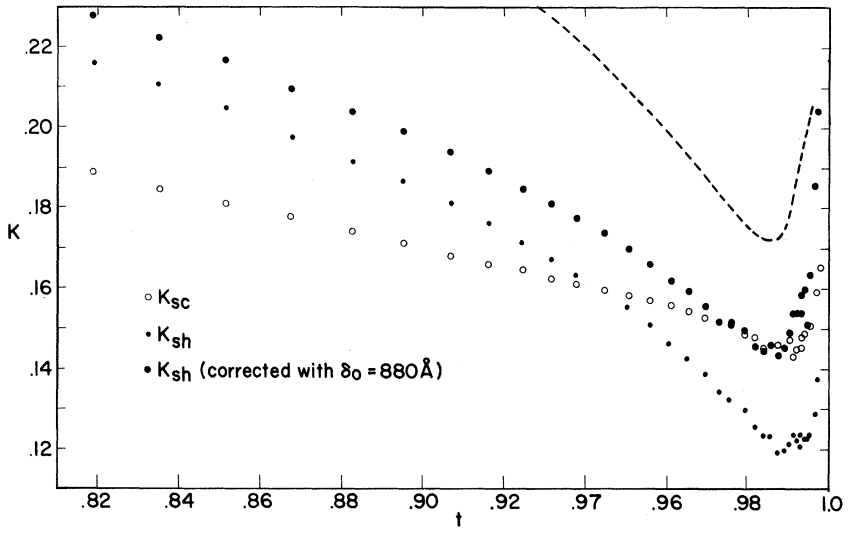

FIG. 15. Superheating and supercooling results for the 11.5-μm β-Ga sphere, when corrections have been made for the effect of the penetration depth and surface depression of the order parameter (see Sec. IV E). New curve for $\kappa_{sh}(t)$ is seen to be lifted considerably as compared with the uncorrected curve. Supercooling points are unchanged, since κ_{sc} is independent of demagnetization factor. Dashed curve is κ_{sh} obtained by using Eq. (15), giving H_{sh} for finite κ in a one-dimensional GL calculation.

we use Eqs. (3) and (10) to get estimates for $\lambda_L(0)$ and ξ_0:

$$\xi_0 = 4860 \pm 600 \text{ Å}, \quad \lambda_L(0) = 710 \pm 100 \text{ Å}.$$

We may get another estimate of ξ_0 by insisting that the size-effect increase in κ_R close to T_c is described by Eq. (13). For the 11.5-μm sphere, the increase becomes noticeable at $T/T_c \sim 0.985$. Inserting this in Eq. (13), we obtain $\xi_0 \sim 2700$ Å, which is lower than the estimate obtained using δ_0, as might be expected.

The transition temperature has been found to be size dependent in other materials.[13] In our experiments on β-Ga single spheres of diameters ranging from 7 to 26 μm, we could see no systematic change of T_c with size.

V. DISCUSSION

The temperature dependence of $H_c(T)$ for β-Ga is that of a strong-coupling superconductor, as the deviation from the parabolic temperature dependence is positive (see Figs. 5 and 6). Using the empirical relationship of Toxen,[37] we find

$$\frac{2\Delta(0)}{kT_c} = -\frac{2T_c}{H_c(0)} \left.\frac{dH_c(T)}{dT}\right|_{T_c} \simeq 4.0 \tag{24}$$

instead of the BCS value 3.56. Cohen *et al.*[38] have studied gallium films in tunneling experiments and found that the phase they identified as the β phase has an energy gap of $\Delta(0) = 1.03$ meV. Fitting the observed $\Delta(T)$ with the BCS expression for $T < 5.5$ K, they determined the transition temperature to be 6.4 K. Thus they found $2\Delta(0)/kT_c = 3.8$. Using our value for T_c with their zero temperature energy gap yields $2\Delta(0)/kT_c = 4.1$, in fair agreement with our result.

From the temperature dependence of $H_c(T)$, we can also obtain the electronic specific-heat coefficient γ, using the empirical relation[39]

$$C_n - C_s = -\frac{T}{4\pi}\left[H_c \frac{d^2H_c}{dT^2} + \left(\frac{dH_c}{dT}\right)^2\right] \to \gamma T, \tag{25}$$

as $T \to 0$. Here C_n and C_s are the electronic specific heats of the normal and the superconducting states, and

$$\gamma = \frac{H_c(0)^2}{2\pi T_c^2}.$$

In Eq. (26) we have neglected the deviation $D(t)$ from the parabolic temperature dependence. Inserting our values for $H_c(0)$ and T_c we find

$$\gamma = 1315 \text{ erg/K}^2 \text{ cm}^3.$$

In the free-electron model one finds

$$\gamma_0 = \tfrac{1}{3} k_B^2 m k_F/\hbar^2 = 875 \text{ erg/K}^2 \text{ cm}^3,$$

where the Fermi wave number k_f was obtained using the density of β-Ga, $\rho_\beta = 6.23 \pm 0.01$ g/cm^3, measured by Bosio *et al.*[28] We thus have

$$\gamma/\gamma_0 = 1.50.$$

In GL theory,[40] using local electrodynamics, the GL parameter may be written

$$\kappa = \frac{\sqrt{2}}{\hbar c} 2e\lambda^2 H_c. \tag{26}$$

Near T_c we have $\lambda \simeq 2^{-1/2}\lambda_L(0)(1-t)^{-1/2}$ and $H_c = H_c(0)(1-t^2) \simeq 2H_c(0)(1-t)$, so that we find

$$\lambda_L(0) = \left(\kappa \frac{\hbar c}{2\sqrt{2}e} \frac{1}{H_c(0)}\right)^{1/2} \approx 242 \text{ Å}, \tag{27}$$

which is much less than the value of $\lambda_L(0) = 765$ Å deduced from the size effects discussed in Sec. IV E.

Although the interpretation of H_{sc} as bulk H_{c3} is expected to be good except in the region very close to T_c, it should be mentioned that Baratoff and

Bergeron[41] have calculated a size dependence of H_{c3} as a function of sphere radius

$$\frac{H_{c3}(R)}{H_{c3}(\infty)} = 1 - 0.65\left(\frac{\xi(T)}{R}\right)^{2/3} + 2.19\,\frac{\xi(T)}{R} + \cdots . \quad (28)$$

Here the last term is the usual size effect treated earlier, giving rise to an apparent increase in κ_{sc} close to T_c. The new term is a negative term on the right-hand side which should give an apparent decrease in κ_{sc} as T_c is approached, competing with the positive term. Assuming, for simplicity, that the bulk GL parameter κ is temperature independent and noticing that $H_{c3}(R)/H_{c3}(\infty) = \kappa_{sc}/\kappa$, we can differentiate Eq. (28) to obtain a minimum in $\kappa_{sc}(t)$ when

$$(1 - t_{min})^{1/2} = 95.4\xi_0/R .$$

Here, we have used $\xi(T) = 0.74\xi_0(1-t)^{-1/2}$. Experimentally, we found $t_{min} = 0.9895$ for the 11.5-μm sphere. Substituting, this yields $\xi_0 \simeq 62$ Å, lower by a factor of 50 than the estimates made from our experimental values of δ_0 and κ. We conclude that Eq. (35) does not describe the size effects in β-Ga. de la Cruz *et al.*[13] reached a similar conclusion from their experiments on Cd.

The superheating results are more difficult to interpret since a number of factors enter into the parametrization of H_{sh}. First of all, we find that the equation for κ_{sh} used so far in interpreting the superheating results, Eq. (14), should be modified in order to take into account the finite penetration depth $\delta(T)$ of the magnetic field. In our present single-sphere experiments, we have shown how the penetration depth $\delta(T)$ may be obtained experimentally (see Sec. IV E). Using the modified expression for κ_{sh} of Eq. (18), we find a substantial correction to the κ_{sh} obtained in the usual way, as seen in Fig. 15.

This effect was not noticed in the earlier single-sphere experiments. This may be due to the fact that δ_0 in In and Sn is somewhat smaller than in β-Ga, and also that the diameters for the spheres used to obtain $\kappa_{sh}(t=1)$ were larger than the 11.5 μm of the β-Ga sphere being discussed here. In fact, a look at the old single-sphere raw data[15] reveals that there is indeed a signal depression close to T_c for these samples also, but smaller than that found for β-Ga, so that for these metals the correction to κ_{sh} would be quite small. We believe, however, that the finite penetration depth effect should give important corrections to the superheating fields obtained in Cd by de la Cruz *et al.*,[13] since their samples range down to 1 μm. In fact, they observe the usual size effect increase in κ_{sc} near T_c; whereas their κ_{sh}, obtained using the spherical demagnetization factor, does not show the usual increase near T_c, but rather a decrease. The smallest spheres, 1 μm in diam, actually show an increase and then a decrease as T_c is approached. Assuming a δ_0 of the same order of magnitude in Cd as in β-Ga, the correction should be very important for the 4- and 1-μm Cd samples, making the κ_{sh} curves exhibit the usual increase as T_c is approached.

Another problem with the superheating field is that the shape of the sample affects the results, also through the demagnetization factor. In single-sphere experiments, one may get an idea of the demagnetization factor by observing H_{sh} as a function of field direction. In the case of In and Sn,[15] all structure in the rotational diagrams vanished near T_c, consistent with a perfect spherical shape. In the present case of β-Ga, the quality of the samples is not as good as for In and Sn, but it seems that the best sample, 11.5 μm in diam, has very little asphericity.

Finally, the interpretation of H_{sh} is complicated by the fact that the existing theory, giving H_{sh} in terms of κ and H_c, describes only the case of one-dimensional fluctuations in the order parameter. As discussed in Sec. II, we expect the Eq. (14) to give the best estimate even in the situation where $\kappa \ll 1$ is not satisfied. The result for finite κ, obtained by Ginzburg and others [see Eq. (15)] certainly represents only an upper limit to H_{sh}. If we use Eqs. (15) and (17) to give κ_{sh}, we obtain the dotted curve in Fig. 15. It is clear that with this correction, the extrapolated value $\kappa_{sh}(T_c)$ is about 10% larger than $\kappa_{sc}(T_c)$. For In and Sn also, $\kappa_{sh}(T_c)$ is larger than $\kappa_{sc}(T_c)$ by about 6–12% if Eq. (15) is used. Thus we consider the present results for κ_{sh} to be about as reliable as those previously obtained on In and Sn, and we believe that κ_{sh} should be calculated using Eq. (18).

Equation (19) gives $H_{sh}(T)$ in the nonlocal limit.[12] In Fig. 16, we have plotted $\frac{3}{2}\kappa^{1/3}(1-t)^{1/12}(H_{sh}/H_c)$ for the β-Ga 11.5-μm sphere. This expression should be temperature independent and equal to 1.36 if Eq. (19) was satisfied. Clearly, the present results are not accurately described by Eq. (19); the factor 1.36 has to be replaced by about 0.8, and there is also a significant temperature variation. Smith *et al.*[12] have found similar results for their In and Sn powder experiments. They also find that the factor 1.36 has to be replaced by ~0.9. Also, they observe a temperature dependence similar to that in Fig. 16.

We find, however, that the presence of flaws increases the temperature dependence of H_{sh}, and it is quite possible that H_{sh} for a perfect sample would satisfy Eq. (19), although with a different constant. At present, with real samples, we do not believe that there is experimental support for Eq. (19).

Finally, we summarize our results for the superconducting properties of β-Ga in Table I.

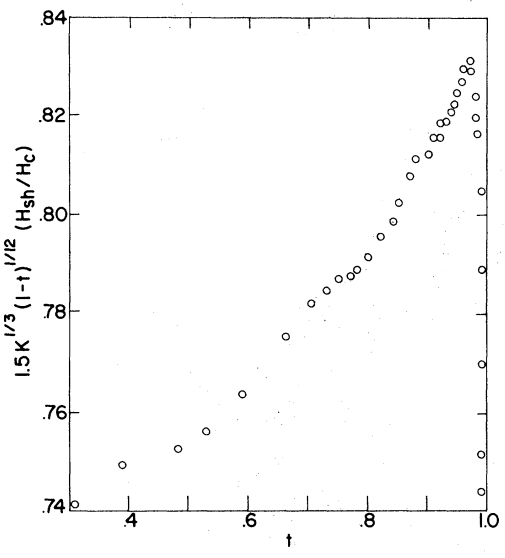

FIG. 16. $\frac{3}{2}\kappa^{1/3}(1-t)^{1/12}(H_{sh}/H_c)$ is plotted vs reduced temperature for the 11.5-μm sphere of β-Ga. According to the derivation of Smith *et al.* [see Eq. (19)], this function should be temperature independent and equal to 1.36.

VI. CONCLUSION

Experimental studies of the superconducting phase transition of small single spheres of metastable β-Ga have been carried out. Both thermodynamic properties and superheating/supercooling were investigated.

In spheres of lesser quality, $H_c(T)$ in some cases exceeded $H_{sh}(T)$, permitting observation of the intermediate state, $H_c(T)$, and the demagnetizing field $H_D(T)$. Size effects were seen close to T_c. We find $T_c = 5.90 \pm 0.03$ K and $H_0 = 538 \pm 5$ Oe. The deviation of $H_c(T)$ from a parabolic temperature dependence is found to be *positive*, having a maximum value $D(t)_{max} = 0.008 \pm 0.003$. This shows that β-Ga is a strong-coupling superconductor, confirming earlier tunneling experiments.[38]

In the best spheres, ideal superheating and supercooling has been observed in a region close to T_c. From extrapolation to $t = 1$ of the supercooling results, we find $\kappa_{GL} = 0.141 \pm 0.002$. A new dimension has been added to this type of experiment by the direct observation of the penetration depth $\delta(T)$ of the magnetic field. This is achieved by studying the variation of the transition signal as a function

TABLE I. Superconductive properties of β-Ga.

T_c, superconductive transition temperature		5.90 ± 0.03 K
$H_c(0)$, thermodynamical critical field at $T = 0$		538 ± 5 Oe
κ, experimental GL parameter at T_c		0.141 ± 0.002
δ_0, experimental zero-temperature penetration depth		880 ± 100 Å
N, number of conduction electrons/cm^3		1.615×10^{23} cm^{-3}
$\gamma = h_c(0)^2/2\pi T_c^2$, electronic specific-heat coefficient		1315 erg/K^2 cm^3
γ_0 = free-electron, electronic specific-heat coefficient		875 erg/K^2 cm^3
γ/γ_0		1.50
$\frac{2\Delta(0)}{kT_c} = \frac{-2T_c}{H_c(0)}\frac{dH_c}{dT}\Big\|_{T=T_c}$		4.0
$\xi_0 = 0.18\,\hbar v_F/k_B T_c$	calculated in free-electron model	4531 Å
$\lambda_L(0) = (mc^2/4\pi Ne^2)^{1/2}$	calculated in free-electron model	132 Å
$\kappa = 0.96\,\lambda_L(0)/\xi_0$	calculated in free-electron model	0.028
$\lambda_L(0) = \left(\frac{2}{\sqrt{3}}\frac{\pi}{0.96}\right)^{1/3}\kappa^{1/3}\delta_0$	estimated using δ_0	710 ± 100 Å
$\xi_0 = 0.96\,\lambda_L(0)/\kappa$	estimated using δ_0	4860 ± 600 Å
$\lambda_L(0)$	estimated from the size effect, Eq. (13)	~400 Å
ξ_0	estimated from the size effect, Eq. (13)	~2700 Å
$\lambda_L(0) = \left(\kappa\frac{(\hbar c/2\sqrt{2}e)}{H_c(0)}\right)^{1/2}$	estimated from $H_c(0)$	240 Å
$\xi_0 = 0.96\,\lambda_L(0)/\kappa$	estimated from $H_c(0)$	1630 Å

of temperature. Using the empirical relation $\delta(T) = \delta_0/(1-t^4)^{1/2}$, which fits the data nicely, we find $\delta_0 = 880 \pm 100$ Å. From the knowledge of this finite penetration depth, we have corrected the spherical demagnetizing factor of $\frac{1}{3}$ used in the interpretation of the superheating data. The resulting change in the parameter κ_{sh} is quite sizeable, amounting to about 17% at $t = 0.99$ for an 11.5-μm sphere. Without this correction, there is clear discrepancy between the extrapolated values of $\kappa_{sc}(t)$ and $\kappa_{sh}(t)$ at $t = 1$. After the correction is made, these extrapolations agree within experimental error, as predicted by one-dimensional GL theory. It is remarkable that the simple low-κ limit calculations of the superheating field [see Eq. (14)] seem to fit the data even for $\kappa = 0.14$. Just as for In and Sn,[15] the numerically calculated values of H_{sh} for intermediate κ [see Eq. (15)] give a clear disagreement between $\kappa_{sh}(t)$ and $\kappa_{sc}(t)$ extrapolated to $t = 1$. We conclude that these calculations overestimate H_{sh}, the best estimate still being Eq. (14).

The independent observation of κ, δ_0, and $H_c(T)$ provides through theoretical relations an overdetermined system of equations to calculate $\lambda_L(0)$ and ξ_0. The size effect observed close to T_c in κ_{sh} and κ_{sc} provides yet another estimate of ξ_0, and thus cross checks are possible. Different sets of values for $\lambda_L(0)$ and ξ_0 were thus calculated using different combinations of the experimental parameters. These estimates agree only within a factor of 3, indicating that the theoretical relations connecting these quantities may have to be refined.

ACKNOWLEDGMENTS

Harald Bratsberg helped us design the cryostat and gave valuable experimental advice. Björn Berling offered countless hours of technical assistance and did all the drawings. We gratefully acknowledge the help of these two and of other members of the Solid State Group at the University of Oslo.

---

*Present address: IBM Thomas J. Watson Research Center, Yorktown Heights, N. Y. 10598.

[1]T. E. Faber, Proc. Roy. Soc. (London) A241, 531 (1957).

[2]J. Feder, S. R. Kiser, and F. Rothwarf, Phys. Rev. Letters 17, 87 (1966).

[3]J. P. Burger, J. Feder, S. R. Kiser, F. Rothwarf, and C. Valette, in *Proceedings of the Tenth International Conference on Low-Temperature Physics*, 1966, edited by M. P. Malkov (Proizvodstrenno-Izdatel'skii Kombinat, VINITI, Moscow, 1967), Vol. 2B, p. 352.

[4]J. Feder, S. R. Kiser, F. Rothwarf, and C. Valette, Solid State Commun 4, 611 (1966).

[5]F. W. Smith and M. Cardona, Phys. Letters 24A, 247 (1967).

[6]H. Bernas, J. P. Burger, G. Deutscher, C. Valette, and S. J. Williamson, Phys. Letters 24A, 721 (1967).

[7]F. W. Smith and M. Cardona, Solid State Commun. 5, 345 (1967).

[8]F. W. Smith, A. Baratoff, and M. Cardona, in *Proceedings of the Eleventh Conference on Low Temperature Physics*, edited by J. F. Allen, D. M. Finlayson, and D. M. McCall (University of St. Andrews Press, St. Andrews, Scotland, 1968), Vol. 2, p. 751.

[9]F. W. Smith and M. Cardona, Solid State Commun. 6, 37 (1968).

[10]F. W. Smith and M. Cardona, Phys. Letters 25A, 671 (1967).

[11]F. de la Cruz, M. D. Maloney, and M. Cardona, in *Superconductivity*, edited by F. Chilton (North-Holland, Amsterdam, 1971), p. 749.

[12]F. W. Smith, A. Baratoff, and M. Cardona, Physik Kondensierten Materie 12, 145 (1970).

[13]F. de la Cruz, M. D. Maloney, and M. Cardona, Phys. Rev. B 3, 3802 (1971).

[14]J. Feder and D. S. McLachlan, Solid State Commun. 6, 23 (1968).

[15]J. Feder and D. S. McLachlan, Phys. Rev. 177, 763 (1969).

[16]F. London, *Superfluids* (Wiley, New York, 1950), p. 35.

[17]See, for instance, the review article by G. Rickayzen, in *Superconductivity*, edited by R. D. Parks (Marcel Dekker, New York, 1969), Vol. 1, pp. 91–93.

[18]V. L. Ginzburg and L. D. Landau, Zh. Eksperim. i Teor. Fiz. 20, 1064 (1950).

[19]V. L. Ginzburg, Zh. Eksperim. i Teor. Fiz. 34, 113 (1958) [Sov. Phys. JETP 7, 78 (1958)].

[20]L. P. Gor'kov, Zh. Eksperim. i Teor. Fiz. 36, 1918 (1959) [Sov. Phys. JETP 9, 1364 (1959)].

[21]L. P. Gor'kov, Zh. Eksperim. i Teor. Fiz. 37, 1407 (1959) [Sov. Phys. JETP 10, 998 (1960)].

[22]D. Saint-James and P. G. de Gennes, Phys. Letters 7, 306 (1963).

[23]J. Feder, Solid State Commun. 5, 299 (1967).

[24]Orsay Group on Superconductivity, in *Quantum Fluids*, edited by D. F. Brewer (North-Holland, Amsterdam, 1966), p. 26.

[25]J. Matricon and D. Saint-James, Phys. Letters 24A, 241 (1967).

[26]V. P. Galaiko, Zh. Eksperim. i Teor. Fiz. 50, 717 (1966) [Sov. Phys. JETP 23, 475 (1966)].

[27]L. Kramer, Phys. Letters 24A, 571 (1967).

[28]L. Bosio, A. Defrain, and I. Épelboin, J. Phys. (Paris) 27, 61 (1966).

[29]L. Bosio, R. Cortès, A. Defrain, and I. Épelboin, Compt. Rend. 264(B), 1592 (1967).

[30]D. S. McLachlan and J. Feder, Rev. Sci. Instr. 39, 1340 (1968).

[31]D. E. Mapother, IBM J. Res. Develop. 6, 77 (1962).

[32]N. E. Phillips, Phys. Rev. 134, A385 (1964).

[33]W. D. Gregory, Phys. Rev. 150, 315 (1966).

[34]J. C. Swihart, IBM J. Res. Develop. 6, 14 (1962).

[35]G. K. Chang and B. Serin, Phys. Rev. 145, 2741 (1966).

[36]See Ref. 15, p. 772.

[37]A. M. Toxen, Phys. Rev. Letters 15, 462 (1965).

[38]R. W. Cohen, B. Abeles, and G. S. Weisbarth,

Phys. Rev. Letters 18, 336 (1967).
[39]R. Meservey and B. B. Schwarz, in Ref. 17, p. 158.
[40]P. G. de Gennes, *Superconductivity of Metals and Alloys* (Benjamin, New York, 1966), p. 182.
[41]A. Baratoff and K. Bergeron, Bull. Am. Phys. Soc. 13, 177 (1968).

PHYSICAL REVIEW B VOLUME 7, NUMBER 1 1 JANUARY 1973

Surface-Plasmon Excitation in Small Spherical Graphite Particles by X Rays*

Christos Koumelis and Dora Leventouri
University of Athens, Physics Laboratory, Athens 144, *Greece*
(Received 6 June 1972)

X-ray scattering experiments have been carried out on dried colloidal graphite, for scattering angles $\varphi = 0°$ and $\varphi = 10°$, using Cr$K\beta_1$ line as a primary radiation. The spectrum for $\varphi = 0°$ shows a faint new component shifted by 13 ± 1 eV from the primary line; the same line was also found for a scattering angle $\varphi = 10°$. If the dried colloidal graphite was replaced by dried colloidal graphite embedded in gelatine, the new component moved to a position shifted by 10 $\pm$ 1 eV from the primary line. The corresponding experiments with polycrystalline graphite did not show such components. These new components can be attributed to a plasmon excitation on the spherical surface of each particle of colloidal graphite. This experiment shows that surface plasmons can be excited in small spherical particles independently of the scattering angle.

I. INTRODUCTION

In recent years, surface plasmons in small spherical particles have been investigated using fast electrons by Kreibig and Zacharias[1] for Ag and Au, by Doremus[2] for Ag and Au, and by Fujimoto and Komaki[3] for Al. Recently, Kokkinakis and Alexopoulos[4] observed surface plasmons in small spherical particles of Ag using x rays.

The study of graphite has received much attention in plasmon investigation because of the two kinds of bulk plasmons, one of low energy (7 eV) due to the π electrons and one of high energy (25 eV) due to π and σ electrons.[5] The existence of both these types of plasmons was established with electron-energy-loss experiments,[6-9] optical measurements,[10] and x-ray-scattering experiments.[11-14]

Recently, the excitation of surface plasmons of colloidal graphite was reported using x-ray techniques.[15] In the present paper a complete report of the experiment is presented. Zero- as well as nonzero-scattering-angle configurations were employed and two different dielectric environments were used for the colloidal-graphite particles.

II. EXPERIMENTAL PROCEDURE

The experimental investigation involves the observation and examination of the transmission spectrum of the radiation produced by a Cr x-ray tube. The radiation was analyzed by a curved-crystal spectrometer and detected by a Geiger counter. The region investigated was the $K\beta_1$ line and the near region towards lower energies. Due to the natural width (3.14 eV) of the line[16] and other experimental limitations, the resolution of the instrument was about 1880. The apparatus has been described in detail elsewhere.[11,17] For the scattering angle $\varphi = 0°$, the following modification was made (Fig. 1): The sample S was positioned just in front of the window of the x-ray tube with its center approximately on the Rowland circle. The scattering angle φ indicated in Refs. 11 and 17 is not shown in Fig. 1 being equal to 0°. It was found that the background was considerably reduced by using a lead shield B. The samples were prepared from colloidal Acheson graphite and were left

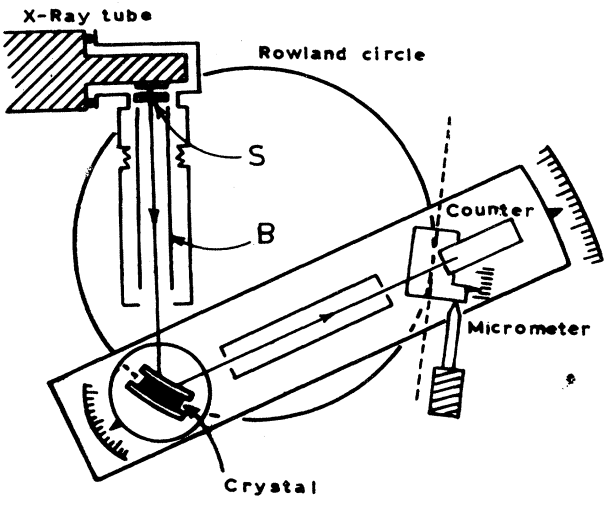

FIG. 1. Experimental set up for $\varphi = 0°$.